The unrestrainable growth of a shear band in a prestressed material
– Electronic supplementary material –

D. Bigoni[1] and F. Dal Corso
Department of Mechanical and Structural Engineering,
University of Trento, via Mesiano 77, I-38050 Trento, Italy
e-mail: bigoni@ing.unitn.it, francesco.dalcorso@ing.unitn.it

1 Introduction

The solution for an inclined crack loaded incrementally under mode I and mode II in a uniformly prestressed, orthotropic incompressible elastic material is obtained together with the incremental energy release rate. The particular cases when the crack is aligned parallel to one of the prestress principal axes and when the crack is inclined, but the prestress is absent, are also explicitly obtained. The effects of prestress are explored in detail on crack fields and growth conditions.

The above results are preliminary to the solution of a shear band, modeled according to the weak line model presented in the paper 'The unrestrainable growth of a shear band in a prestressed material', loaded under incremental mode II (while mode I loading leaves the material unperturbed) and embedded in a uniformly prestressed, orthotropic and incompressible nonlinear elastic material.

2 Incremental constitutive equations for incompressible nonlinear elasticity

According to the Biot (1965) theory, the response of a nonlinear elastic, incompressible and uniformly deformed material subjected to an incremental loading is expressed in terms of the nominal (unsymmetrical) stress increment $\dot{\mathbf{t}}$, related to the gradient of incremental displacement $\nabla \mathbf{v}$ (satisfying the incompressibility constraint $\mathrm{tr}\nabla\mathbf{v} = 0$) through the linear relation

$$\dot{\mathbf{t}} = \mathbb{K}[\nabla \mathbf{v}^T] + \dot{p}\,\mathbf{I}, \tag{1}$$

[1]Corresponding author: Davide Bigoni fax: +39 0461 882599; tel.: +39 0461 882507; web-site: http://www.ing.unitn.it/∼bigoni/; e-mail: bigoni@ing.unitn.it.

where T denotes the transpose, $\dot{p}$ is the incremental in-plane mean stress and the components of constitutive fourth-order tensor $\mathbb{K}$ (possessing the major symmetry $\mathbb{K}_{ijhk} = \mathbb{K}_{hkij}$) are:

$$\begin{aligned}
&\mathbb{K}_{1111} = \mu(\xi - k - \eta), && \mathbb{K}_{1122} = -\mu\,\xi, && \mathbb{K}_{1112} = \mathbb{K}_{1121} = 0,\\
&\mathbb{K}_{2211} = -\mu\,\xi, && \mathbb{K}_{2222} = \mu(\xi + k - \eta), && \mathbb{K}_{2212} = \mathbb{K}_{2221} = 0,\\
&\mathbb{K}_{1212} = \mu(1 + k), && \mathbb{K}_{1221} = \mathbb{K}_{2112} = \mu(1 - \eta), && \mathbb{K}_{2121} = \mu(1 - k).
\end{aligned} \tag{2}$$

The components of the constitutive fourth-order tensor $\mathbb{K}$ depend on the current state of stress (expressed through the principal components of Cauchy stress, σ_1 and σ_2) and material response to shear (μ for shear parallel and μ_* for shear inclined at $\pi/4$ with respect to σ_1) describing orthotropy (aligned parallel to the current principal stress directions), see Bigoni and Capuani (2002, 2005) for details, through the dimensionless quantities:

$$\xi = \frac{\mu_*}{\mu}, \qquad \eta = \frac{\sigma_1 + \sigma_2}{2\mu}, \qquad k = \frac{\sigma_1 - \sigma_2}{2\mu}. \tag{3}$$

Positive definiteness of $\mathbb{K}$

The Hill exclusion condition for bifurcation (Hill, 1958) is the condition of positive definiteness of the constitutive fourth-order tensor $\mathbb{K}$ [Hill and Hutchinson, 1975, their eqn. (3.9)]. Assuming $\mu > 0$, in terms of dimensionless constants (3), this condition becomes

$$0 < \eta < 2\xi, \quad \frac{k^2 + \eta^2}{2\eta} < 1, \tag{4}$$

defining a region in the space ξ, k and η, which bound has been reported in Fig. 1 for different values of η/k.

Regime classification

Since the material response described by eqn. (1) is incompressible, we can introduce a *stream function* $\psi(x_1, x_2)$, with the property (where a comma means differentiation with respect to the corresponding spatial variable)

$$v_1 = \psi_{,2}, \qquad v_2 = -\psi_{,1}, \tag{5}$$

so that the incompressibility constraint is automatically satisfied. Assuming zero body forces, the elimination of $\dot{p}$ in the incremental equilibrium equations ($\dot{t}_{ij,i} = 0$) gives the fourth-order partial differential equation

$$(1 + k)\psi_{,1111} + 2(2\xi - 1)\psi_{,1122} + (1 - k)\psi_{,2222} = 0, \tag{6}$$

derived by Biot [1965, pp. 193, his eqn. (3.7), see also Hill and Hutchinson, 1975, their eqn. (3.3)].

Following Lekhnitskii (1981), Guz (1999), Cristescu *et al.* (2004), Radi *et al.* (2002) and Dal Corso *et al.* (2008), a solution of (6) can be represented in terms of the analytic function F

$$\psi(x_1, x_2) = F(x_1 + \Omega x_2), \tag{7}$$

where Ω is a complex constant satisfying the biquadratic equation obtained inserting representation (7) in eqn. (6)

$$1 + k + 2(2\xi - 1)\Omega^2 + (1 - k)\Omega^4 = 0. \tag{8}$$

The four roots Ω_j $(j = 1, \ldots, 4)$ of eqn. (8) satisfy

$$\Omega_j^2 = \frac{1 - 2\xi + (-1)^j \Lambda}{1 - k}, \tag{9}$$

where

$$\Lambda = \sqrt{4\xi^2 - 4\xi + k^2}, \tag{10}$$

and are real or complex depending on the values of ξ and k. In compact form, we write

$$\Omega_j = \alpha_j + i\beta_j, \qquad j = 1, \ldots, 4, \tag{11}$$

and define the four complex variables

$$z_j = x_1 + \Omega_j x_2 = x_1 + \alpha_j x_2 + i\beta_j x_2 \qquad j = 1, \ldots, 4, \tag{12}$$

where $i = \sqrt{-1}$ is the imaginary unit and $\alpha_j = \mathrm{Re}[\Omega_j]$ and $\beta_j = \mathrm{Im}[\Omega_j]$.

Employing eqns. (7) and (12), *the general solution of the differential eqn.* (6) can be written as

$$\psi(x_1, x_2) = \sum_{j=1}^{4} F_j(z_j). \tag{13}$$

The roots Ω_j, defined by eqn. (9), change their nature according to the values of parameters ξ and k, so that the differential equation (6) can be classified as reported by Dal Corso *et al.* (2008). The regime classification in the $k - \xi$ plane has been given by Radi *et al.* (2002) and is sketched in Fig. 1.

In the elliptic imaginary regime (EI), defined as

$$k^2 < 1 \quad \text{and} \quad 2\xi > 1 + \sqrt{1 - k^2}, \tag{14}$$

we have four imaginary conjugate roots Ω_j, so that

$$\alpha_1 = \alpha_2 = 0, \qquad \left.\begin{matrix}\beta_1 \\ \beta_2\end{matrix}\right\} = \sqrt{\frac{2\xi - 1 \pm \sqrt{4\xi^2 - 4\xi + k^2}}{1 - k}} > 0, \tag{15}$$

while in the elliptic complex regime (EC), defined as

$$k^2 < 1 \quad \text{and} \quad 1 - \sqrt{1 - k^2} < 2\xi < 1 + \sqrt{1 - k^2}, \tag{16}$$

we have four complex conjugate roots Ω_j, so that

$$\left.\begin{matrix}\beta = \beta_1 = \beta_2 \\ \alpha = -\alpha_1 = \alpha_2\end{matrix}\right\} = \sqrt{\frac{\sqrt{1 - k^2} \pm (2\xi - 1)}{2(1 - k)}} > 0. \tag{17}$$

Specific cases of material behaviour

The assumption of a specific material model determines the relation between ξ and k. For instance, a Mooney-Rivlin material coincides with a neo-Hookean material for plane isochoric deformations, so that parameters k and ξ become (where λ is the logarithmic stretch, representing a prestrain measure)

$$k = \frac{\lambda^2 - \lambda^{-2}}{\lambda^2 + \lambda^{-2}}, \quad \xi = 1, \tag{18}$$

while for a J_2–deformation theory material (Hutchinson and Neale, 1979), particularly suited to analyse the plastic branch of the constitutive response of ductile metals, we have

$$k = \frac{\lambda^4 - 1}{\lambda^4 + 1}, \quad \xi = \frac{N(\lambda^4 - 1)}{2(\ln \lambda)\,(\lambda^4 + 1)}, \tag{19}$$

where N is the hardening exponent. The curve in the ξ versus k plane described by eqn. (19) for $N = 0.3$ is reported in Fig. 2 of the paper.

Shear bands inclination

At the EC/H boundary *two* shear bands become simultaneously possible, their inclinations are given by the angles $\pm\vartheta_0$ between the shear band and the x_1–axis and solution of (Hill and Hutchinson, 1975)

$$\cot^2 \vartheta_0 = \frac{1 + 2\,\mathrm{sign}(k)\sqrt{\xi\,(1-\xi)}}{1 - 2\xi}. \tag{20}$$

At the EI/P boundary, we have only *one* shear band possible aligned parallel to the x_1–axis (x_2–axis), when $k = 1$ ($k = -1$)

$$\vartheta_0 = 0, \quad \text{for } k = 1, \quad \text{or} \quad \vartheta_0 = \frac{\pi}{2}, \quad \text{for } k = -1. \tag{21}$$

Surface bifurcation

Surface instability occurs [Needleman and Ortiz, 1991, their eqn. (48)] when

$$4\xi - 2\eta = \frac{\eta^2 - 2\eta + k^2}{\sqrt{1-k^2}}, \tag{22}$$

which, in the particular case of stress parallel to the free surface $x_1 = 0$ ($\eta = k$), becomes

$$\xi = \frac{k}{2}\left(1 - \sqrt{\frac{1-k}{1+k}}\right). \tag{23}$$

Surface bifurcation, eqn. (22), and the Hill exclusion condition, eqn. (4), are reported in Fig. 1 for different values of η/k .

In our model of shear band, a sliding surface abruptly (but affecting only incremental fields) forms when the thin layer of material representing the shear band touches the elliptic boundary, while in a refined modelling, a weak thin layer of material should approach the elliptic boundary becoming incrementally less and less stiff in a continuous way. The abrupt formation of a sliding

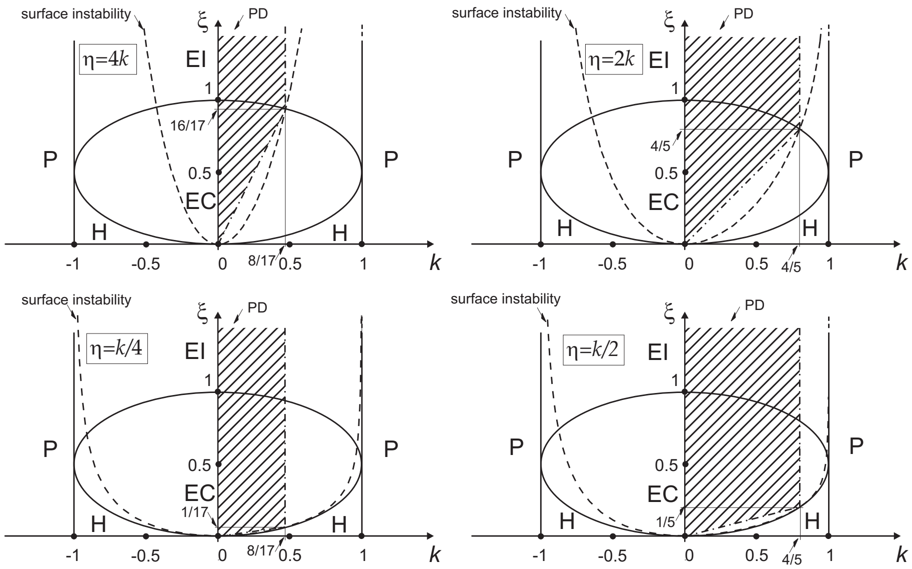

Figure 1: Surface bifurcation for $\eta = \{4k, 2k, k/4, k/2\}$ and the Hill exclusion condition, eqn. (4), in the $\xi = \mu_*/\mu$ versus $k = (\sigma_1 - \sigma_2)/2$ parameter space, reported with the regime classification.

surface within an infinite solid may, depending on the stress conditions, generate a sudden 'spurious' interfacial instability, so that in this condition our shear band model becomes oversimplified. Therefore, the model has to be employed only in situations where surface instabilities are a-priori excluded until the elliptic boundary is met, a circumstance that can be attained employing the Hill (1958) exclusion condition, see also Hill and Hutchinson [1975, their eqn. (3.9)]. However, this condition is so general that all points of the EC/H and EI/P boundaries can be explored, by taking $k > 0$ and selecting appropriate values for the prestress parameter η, as can be noted from Fig. 1.

3 Finite-length crack in a prestressed material

A homogenously prestressed and prestrained, incompressible elastic infinite plane is considered, characterized by the constitutive equation (1) of incremental, incompressible, orthotropic elasticity, containing a crack of current length $2l$, taken parallel to the $\hat{x}_1$-axis in the $\hat{x}_1$–$\hat{x}_2$ reference system, and loaded at infinity by a uniform nominal stress increment $\hat{t}^{\infty}_{2n}$, where $n = 1$ corresponds to mode II and $n = 2$ to mode I loading, see Fig. 2.

Obviously, the crack faces cannot be free of tractions, since a dead loading is required to 'provide' the prestress state (with principal Cauchy components σ_1 and σ_2, assumed aligned parallel to the x_1–x_2 reference system, rotated at an angle ϑ_0 with respect to the $\hat{x}_1$–$\hat{x}_2$ system). An interesting exception to this rule occurs when the crack is aligned parallel to the x_1-axis and the prestress is aligned parallel to the crack surfaces, namely when the $\hat{x}_1$–$\hat{x}_2$ and x_1–x_2 systems coincide, i.e. $\vartheta_0 = 0$, and $\sigma_2 = 0$, corresponding to $\eta = k$. This

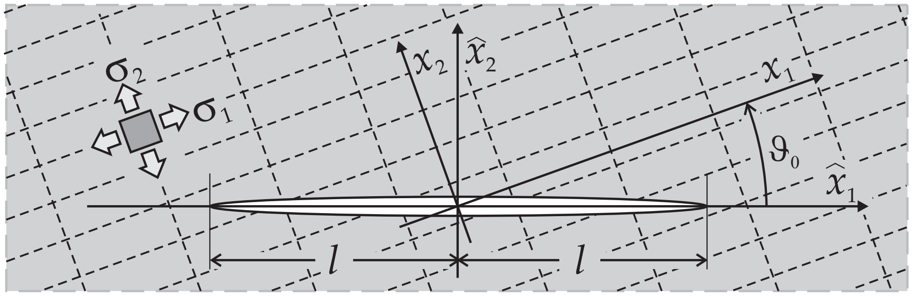

Figure 2: Finite-length ($2l$) crack in a prestressed, orthotropic material inclined at an angle ϑ_0 (positive when anticlockwise) with respect to the orthotropy axes x_1 and x_2.

situation has been considered by Guz (1999, and references quoted therein), Cristescu *et al.* (2004) and Radi *et al.* (2002, in the near-tip asymptotic limit). The case of a generic inclination ϑ_0, has never been treated in the case of a prestressed material, but it is well-known in linear, infinitesimal, anisotropic elasticity (Savin, 1961; see also Sih and Liebowitz, 1968).

Solution to the above-formulated crack problem is obtained by superimposing the trivial, unperturbed solution to the perturbation induced by the crack, the latter denoted with the apex $\circ$.

The unperturbed solutions are obtained defining the uniform nominal stress field in the $\hat{x}_1$–$\hat{x}_2$ reference system

$$\hat{t}_{22} = \hat{t}_{22}^{\infty}, \quad \hat{t}_{11} = 0, \quad \hat{t}_{12} = \hat{t}_{21} = \hat{t}_{21}^{\infty}, \tag{24}$$

so that $\hat{t}_{21}^{\infty} = 0$ ($\hat{t}_{22}^{\infty} = 0$) for mode I (mode II).

The nominal stress increment, incremental displacement and its gradient in the $\hat{x}_1$–$\hat{x}_2$ reference system can be obtained through a rotation of the components in the prestress principal reference system x_1–x_2. Since the two systems are rotated at an angle ϑ_0 (taken positive when anticlockwise), we have

$$\hat{\mathbf{x}} = \mathbf{Q}^T\mathbf{x}, \quad [\mathbf{Q}] = \left[\begin{array}{cc} \cos\vartheta_0 & \sin\vartheta_0 \\ -\sin\vartheta_0 & \cos\vartheta_0 \end{array}\right], \tag{25}$$

so that the nominal stress increment, incremental displacement and its gradient can be expressed in the $\hat{x}_1$–$\hat{x}_2$ reference system as

$$\hat{\dot{\mathbf{t}}} = \mathbf{Q}^T\dot{\mathbf{t}}\mathbf{Q}, \quad \hat{\mathbf{v}} = \mathbf{Q}^T\mathbf{v}, \quad \hat{\nabla}\hat{\mathbf{v}} = \mathbf{Q}^T\nabla\mathbf{v}\mathbf{Q}, \tag{26}$$

while the constitutive equation (1) transforms to

$$\hat{\dot{\mathbf{t}}} = \widehat{\mathbb{K}}[\hat{\nabla}\hat{\mathbf{v}}^T] + \dot{p}\,\mathbf{I}, \tag{27}$$

where the transformed fourth-order tensor $\widehat{\mathbb{K}}$ is given by

$$\widehat{\mathbb{K}}_{ijhk} = Q_{li}Q_{mj}\mathbb{K}_{lmno}Q_{nh}Q_{ok}. \tag{28}$$

Note that the above definition (24) of mode I and II loadings is fully meaningful only when the constitutive equations (1) are positive defined, so that the

Hill exclusion condition (4) holds true. For a non-positive definite constitutive equation, definition (24) would be better changed to one concerning the components of the incremental displacement gradient.

Assuming that condition (4) holds true, we can directly obtain from eqns. (1), (2) and $(26)_1$ the components of the incremental displacement gradient and the incremental in-plane mean stress in the x_1–x_2 reference system

$$
\begin{aligned}
\dot{p} &= \frac{\hat{t}_{22}^{\infty}}{2} - \mu k v_{2,2}, \\
v_{2,2} = -v_{1,1} &= \frac{\hat{t}_{22}^{\infty}\cos 2\vartheta_0 - 2\hat{t}_{21}^{\infty}\sin 2\vartheta_0}{2\mu(2\xi-\eta)}, \\
v_{1,2} &= -\frac{(k+\eta)\left(\hat{t}_{22}^{\infty}\sin 2\vartheta_0 + 2\hat{t}_{21}^{\infty}\cos 2\vartheta_0\right)}{2\mu(k^2-2\eta+\eta^2)}, \\
v_{2,1} &= \frac{(k-\eta)\left(\hat{t}_{22}^{\infty}\sin 2\vartheta_0 + 2\hat{t}_{21}^{\infty}\cos 2\vartheta_0\right)}{2\mu(k^2-2\eta+\eta^2)}.
\end{aligned}
\tag{29}
$$

The components of the incremental displacement gradient in the $\hat{x}_1$–$\hat{x}_2$ reference system can be obtained through a rotation of eqns. (29), by employing eqn. $(26)_3$.

It should be noted from eqns. (29) that in the absence of prestress, $k = \eta = 0$, eqns. (29) fully determine the incremental displacement gradient. However, in this case, the incremental stress is only related to the symmetric part of the incremental displacement gradient, so that an arbitrary incremental rotation can be added without altering the state of stress, a circumstance not possible when the prestress is different from zero. In other words, when the prestress is present, loading (24) completely defines the incremental displacement gradient (and incremental mean stress) through eqns. (29), so that incremental rigid body rotations remain determined.

3.1 Finite-length crack parallel to an orthotropy axis

Before proceeding with the solution of the inclined crack, it becomes instructive to begin with the simple case of null inclination, in which $\vartheta_0 = 0$, so that the orthotropy axes are aligned parallel and orthogonal to the x_1–x_2 axes, defining the prestress directions and coinciding with the $\hat{x}_1$–$\hat{x}_2$ axes.

The perturbed solution is derived separately for the two EI and EC regimes (beginning with EI). The stream function ψ°, eqn. (5), can be represented in the form (note that the summation ranges between 1 and 2, since the Ω_j's are in conjugated pairs in the elliptic regime)

$$
\psi^{\circ}(z_1, z_2) = \mathrm{Re}\left[\sum_{j=1}^{2} F_j(z_j)\right], \tag{30}
$$

where $z_j = x_1 + \Omega_j x_2$, with Ω_j given by eqn. (9), so that the displacement field becomes

$$v_1^\circ(z_1,z_2) = \mathrm{Re}\left[\sum_{j=1}^{2} \Omega_j F_j'(z_j)\right], \qquad v_2^\circ(z_1,z_2) = -\mathrm{Re}\left[\sum_{j=1}^{2} F_j'(z_j)\right], \tag{31}$$

and its gradient can be written as

$$\begin{aligned} v_{1,1}^\circ(z_1,z_2) &= -v_{2,2}^\circ(z_1,z_2) = \mathrm{Re}\left[\sum_{j=1}^{2} \Omega_j F_j''(z_j)\right], \\ v_{1,2}^\circ(z_1,z_2) &= \mathrm{Re}\left[\sum_{j=1}^{2} \Omega_j^2 F_j''(z_j)\right], \quad v_{2,1}^\circ(z_1,z_2) = -\mathrm{Re}\left[\sum_{j=1}^{2} F_j''(z_j)\right]. \end{aligned} \tag{32}$$

The effects of the applied boundary conditions on the crack surfaces decay to zero at infinity, so that, from eqns. (32) and the constitutive relation (1) we obtain

$$\lim_{|z_j|\to+\infty} F_j''(z_j) = 0, \qquad j = 1,2. \tag{33}$$

Mode I

To recover traction-free crack faces using superposition, the incremental nominal stress component $\dot{t}_{22}^\infty$ of reversed sign has to be prescribed at crack surfaces in the perturbed problem, namely for mode I

$$\begin{aligned} \dot{t}_{22}^\circ(x_1,0^\pm) &= -\dot{t}_{22}^\infty \qquad \forall\,|x_1| < l, \\ \dot{t}_{21}^\circ(x_1,0^\pm) &= 0, \qquad\quad \forall\, x_1 \in \mathbb{R}. \end{aligned} \tag{34}$$

From eqns. $(34)_2$ and (32) the following relation can be obtained, holding at every point x_1 of the real axis $\mathbb{R}$

$$F_2''(x_1) = -\frac{2\xi - \eta + \Lambda}{2\xi - \eta - \Lambda} F_1''(x_1), \tag{35}$$

where Λ is defined by eqn. (10), while from eqn. $(34)_1$ the condition

$$\frac{\dot{t}_{22}^\infty}{\mu} = \sum_{j=1}^{2} \mathrm{Re}\left\{\Omega_j \left[4\xi - 1 - \eta + \Omega_j^2(1-k)\right] F_j''(x_1)\right\}, \tag{36}$$

follows, to hold true along the crack line $|x_1| < l$.

Within the EI regime, eqns. (14), and for mode I, the Riemann-Hilbert problem:

$$-\frac{\beta_2\varepsilon_1^2 - \beta_1\varepsilon_2^2}{\varepsilon_2}\mathrm{Re}\left[iF_1''(x_1)\right] = \frac{\dot{t}_{22}^\infty}{\mu}, \qquad \forall\,|x_1| < l, \tag{37}$$

where β_1 and β_2 are defined by eqn. (15) and

$$\varepsilon_n = 1 - \eta + (1-k)\beta_n^2, \quad n = 1,2, \tag{38}$$

has the following solution:

$$F_j''(z_j) = (-1)^k i \frac{\dot{t}_{22}^{\infty}}{\mu} \frac{\varepsilon_k}{\beta_2 \varepsilon_1^2 - \beta_1 \varepsilon_2^2} \left(1 - \frac{z_j}{\sqrt{z_j^2 - l^2}} \right), \quad j,k = 1,2, \quad j \neq k. \quad (39)$$

The perturbed stream function becomes

$$\psi^{\circ} = -\frac{\dot{t}_{22}^{\infty}}{2\mu} \frac{\varepsilon_2}{\beta_2 \varepsilon_1^2 - \beta_1 \varepsilon_2^2} \sum_{j=1}^{2} \left(-\frac{\varepsilon_1}{\varepsilon_2} \right)^{j-1} \mathrm{Im} \left\{ z_j^2 - z_j \sqrt{z_j^2 - l^2} + l^2 \ln \left(z_j + \sqrt{z_j^2 - l^2} \right) \right\}, \quad (40)$$

and the incremental displacements take the form

$$v_1^{\circ} = -\frac{\dot{t}_{22}^{\infty}}{\mu} \frac{\varepsilon_2}{\beta_2 \varepsilon_1^2 - \beta_1 \varepsilon_2^2} \mathrm{Re} \left[\beta_1 \left(z_1 - \sqrt{z_1^2 - l^2} \right) - \frac{\beta_2 \varepsilon_1}{\varepsilon_2} \left(z_2 - \sqrt{z_2^2 - l^2} \right) \right],$$

$$v_2^{\circ} = \frac{\dot{t}_{22}^{\infty}}{\mu} \frac{\varepsilon_2}{\beta_2 \varepsilon_1^2 - \beta_1 \varepsilon_2^2} \mathrm{Im} \left[\left(z_1 - \sqrt{z_1^2 - l^2} \right) - \frac{\varepsilon_1}{\varepsilon_2} \left(z_2 - \sqrt{z_2^2 - l^2} \right) \right]. \quad (41)$$

Finally, for mode I in the EI regime, the incremental in-plane mean stress is given by

$$\dot{p}^{\circ} = \frac{\dot{t}_{22}^{\infty} \varepsilon_2}{\beta_2 \varepsilon_1^2 - \beta_1 \varepsilon_2^2} \left\{ \frac{\varepsilon_2 \beta_1 \delta_1 - \varepsilon_1 \beta_2 \delta_2}{\varepsilon_2} - \mathrm{Re} \left[\beta_1 \delta_1 \frac{z_1}{\sqrt{z_1^2 - l^2}} - \frac{\varepsilon_1 \beta_2 \delta_2}{\varepsilon_2} \frac{z_2}{\sqrt{z_2^2 - l^2}} \right] \right\}, \quad (42)$$

where

$$\delta_n = 2\xi - 1 - k - (1-k)\beta_n^2, \quad n = 1,2, \quad (43)$$

while the incremental nominal stress components are

$$\dot{t}_{11}^{\circ} = -\dot{t}_{22}^{\infty} \frac{\varepsilon_1 \varepsilon_2}{\beta_2 \varepsilon_1^2 - \beta_1 \varepsilon_2^2} \left\{ \beta_1 - \beta_2 - \mathrm{Re} \left[\beta_1 \frac{z_1}{\sqrt{z_1^2 - l^2}} - \beta_2 \frac{z_2}{\sqrt{z_2^2 - l^2}} \right] \right\},$$

$$\dot{t}_{22}^{\circ} = -\dot{t}_{22}^{\infty} \left\{ 1 + \frac{\varepsilon_2}{\beta_2 \varepsilon_1^2 - \beta_1 \varepsilon_2^2} \mathrm{Re} \left[\beta_1 \varepsilon_2 \frac{z_1}{\sqrt{z_1^2 - l^2}} - \frac{\varepsilon_1^2 \beta_2}{\varepsilon_2} \frac{z_2}{\sqrt{z_2^2 - l^2}} \right] \right\},$$

$$\dot{t}_{12}^{\circ} = -\dot{t}_{22}^{\infty} \frac{\varepsilon_2}{\beta_2 \varepsilon_1^2 - \beta_1 \varepsilon_2^2} \mathrm{Im} \left[\beta_1^2 \varepsilon_2 \frac{z_1}{\sqrt{z_1^2 - l^2}} - \frac{\varepsilon_1^2 \beta_2^2}{\varepsilon_2} \frac{z_2}{\sqrt{z_2^2 - l^2}} \right],$$

$$\dot{t}_{21}^{\circ} = -\dot{t}_{22}^{\infty} \frac{\varepsilon_1 \varepsilon_2}{\beta_2 \varepsilon_1^2 - \beta_1 \varepsilon_2^2} \mathrm{Im} \left[\frac{z_1}{\sqrt{z_1^2 - l^2}} - \frac{z_2}{\sqrt{z_2^2 - l^2}} \right]. \quad (44)$$

Within the EC regime, eqns. (16), and for mode I, the Riemann-Hilbert problem:

$$2 \left[\alpha(\delta^2 - \chi^2) + 2\beta\delta\chi \right] \mathrm{Re} \left[\frac{F_1''(x_1)}{\chi - i\delta} \right] = \frac{\dot{t}_{22}^{\infty}}{\mu}, \qquad \forall |x_1| < l, \quad (45)$$

where α and β are defined by eqn. (17) and

$$\delta = 2(1-k)\alpha\beta, \quad \chi = 2\xi - \eta, \tag{46}$$

has the following solution:

$$F_j''(z_j) = (-1)^k \frac{\dot{t}_{22}^{\infty}}{2\mu} \frac{\chi + (-1)^j i\delta}{\alpha(\delta^2-\chi^2)+2\beta\delta\chi} \left(1 - \frac{z_j}{\sqrt{z_j^2 - l^2}}\right), \quad j,k = 1,2, \quad j \neq k. \tag{47}$$

The perturbed stream function becomes

$$\begin{aligned} \psi^{\circ} &= -\frac{\dot{t}_{22}^{\infty}}{4\mu[\alpha(\delta^2-\chi^2)+2\beta\delta\chi]} \sum_{j=1}^{2} \mathrm{Re}\left\{\left[(-1)^j\chi + i\delta\right]\right. \\ &\quad \times \left.\left[z_j^2 - z_j\sqrt{z_j^2-l^2} + l^2 \ln\left(z_j + \sqrt{z_j^2-l^2}\right)\right]\right\}, \end{aligned} \tag{48}$$

and the incremental displacements take the form

$$\begin{aligned} v_1^{\circ} &= -\frac{\dot{t}_{22}^{\infty}}{2\mu} \frac{1}{\alpha(\delta^2-\chi^2)+2\beta\delta\chi} \left\{(\alpha\chi - \beta\delta)\,\mathrm{Re}\left[\left(z_1 - \sqrt{z_1^2-l^2}\right) + \left(z_2 - \sqrt{z_2^2-l^2}\right)\right]\right. \\ &\quad \left. + (\alpha\delta + \beta\chi)\,\mathrm{Im}\left[\left(z_1 - \sqrt{z_1^2-l^2}\right) - \left(z_2 - \sqrt{z_2^2-l^2}\right)\right]\right\}, \\ v_2^{\circ} &= -\frac{\dot{t}_{22}^{\infty}}{2\mu} \frac{1}{\alpha(\delta^2-\chi^2)+2\beta\delta\chi} \left\{\chi\,\mathrm{Re}\left[\left(z_1 - \sqrt{z_1^2-l^2}\right) - \left(z_2 - \sqrt{z_2^2-l^2}\right)\right]\right. \\ &\quad \left. + \delta\,\mathrm{Im}\left[\left(z_1 - \sqrt{z_1^2-l^2}\right) + \left(z_2 - \sqrt{z_2^2-l^2}\right)\right]\right\}. \end{aligned} \tag{49}$$

Finally, for mode I in the EC regime, the incremental in-plane mean stress is given by

$$\begin{aligned} \dot{p}^{\circ} &= -\frac{\dot{t}_{22}^{\infty}}{2} \frac{1}{\alpha(\delta^2-\chi^2)+2\beta\delta\chi} \\ &\quad \times \left\{[(\beta\chi+\alpha\delta)\delta + (\alpha\chi-\beta\delta)k]\left(2 - \mathrm{Re}\left[\frac{z_1}{\sqrt{z_1^2-l^2}} + \frac{z_2}{\sqrt{z_2^2-l^2}}\right]\right)\right. \\ &\quad \left. - [(\beta\chi+\alpha\delta)k - (\alpha\chi-\beta\delta)\delta]\,\mathrm{Im}\left[\frac{z_1}{\sqrt{z_1^2-l^2}} - \frac{z_2}{\sqrt{z_2^2-l^2}}\right]\right\}, \end{aligned} \tag{50}$$

while the incremental nominal stress components are

$$\begin{aligned} \dot{t}_{11}^{\circ} &= -\frac{\dot{t}_{22}^{\infty}}{2} \frac{\delta^2+\chi^2}{\alpha(\delta^2-\chi^2)+2\beta\delta\chi} \left\{2\alpha - \alpha\,\mathrm{Re}\left[\frac{z_1}{\sqrt{z_1^2-l^2}} + \frac{z_2}{\sqrt{z_2^2-l^2}}\right]\right. \\ &\quad \left. - \beta\,\mathrm{Im}\left[\frac{z_1}{\sqrt{z_1^2-l^2}} - \frac{z_2}{\sqrt{z_2^2-l^2}}\right]\right\}, \\ \dot{t}_{22}^{\circ} &= -\frac{\dot{t}_{22}^{\infty}}{2} \left\{2 - \mathrm{Re}\left[\frac{z_1}{\sqrt{z_1^2-l^2}} + \frac{z_2}{\sqrt{z_2^2-l^2}}\right]\right. \\ &\quad \left. - \frac{\beta(\delta^2-\chi^2)-2\alpha\delta\chi}{\alpha(\delta^2-\chi^2)+2\beta\delta\chi}\,\mathrm{Im}\left[\frac{z_1}{\sqrt{z_1^2-l^2}} - \frac{z_2}{\sqrt{z_2^2-l^2}}\right]\right\}, \\ \dot{t}_{12}^{\circ} &= \frac{\dot{t}_{22}^{\infty}}{2} \left\{\frac{(\alpha^2-\beta^2)(\delta^2-\chi^2)+4\alpha\beta\delta\chi}{\alpha(\delta^2-\chi^2)+2\beta\delta\chi}\,\mathrm{Re}\left[\frac{z_1}{\sqrt{z_1^2-l^2}} - \frac{z_2}{\sqrt{z_2^2-l^2}}\right]\right. \\ &\quad \left. + \frac{2\alpha\beta(\delta^2-\chi^2)-2\delta\chi(\alpha^2-\beta^2)}{\alpha(\delta^2-\chi^2)+2\beta\delta\chi}\,\mathrm{Im}\left[\frac{z_1}{\sqrt{z_1^2-l^2}} + \frac{z_2}{\sqrt{z_2^2-l^2}}\right]\right\}, \\ \dot{t}_{21}^{\circ} &= \frac{\dot{t}_{22}^{\infty}}{2} \frac{\delta^2+\chi^2}{\alpha(\delta^2-\chi^2)+2\beta\delta\chi}\,\mathrm{Re}\left[\frac{z_1}{\sqrt{z_1^2-l^2}} - \frac{z_2}{\sqrt{z_2^2-l^2}}\right]. \end{aligned} \tag{51}$$

Mode II

The reverse of the incremental nominal stress component $\dot{t}_{21}^{\infty}$ has to be applied at the crack surfaces in the perturbed mode II solution, namely

$$\begin{aligned} \dot{t}_{22}^{\circ}(x_1, 0^{\pm}) &= 0, & \forall\, x_1 \in \mathbb{R}, \\ \dot{t}_{21}^{\circ}(x_1, 0^{\pm}) &= -\dot{t}_{21}^{\infty}, & \forall\, |x_1| < l. \end{aligned} \tag{52}$$

Eqns. $(52)_1$, (32) and eqn. $(52)_2$ provide the two conditions,

$$F_2''(x_1) = -\frac{\Omega_1}{\Omega_2}\frac{2\xi - \eta - \Lambda}{2\xi - \eta + \Lambda} F_1''(x_1), \tag{53}$$

holding at every point x_1 of the real axis $\mathbb{R}$ and

$$\frac{\dot{t}_{21}^{\infty}}{\mu} = \sum_{j=1}^{2} \mathrm{Re}\left\{ \left[1 - \eta - \Omega_j^2(1-k)\right] F_j''(x_1) \right\}, \tag{54}$$

holding for $|x_1| < l$.

Within the EI regime, eqns. (14), and for mode II, the Riemann-Hilbert problem:

$$\frac{\beta_2 \varepsilon_1^2 - \beta_1 \varepsilon_2^2}{\beta_2 \varepsilon_1} \mathrm{Re}\left[F_1''(x_1)\right] = \frac{\dot{t}_{21}^{\infty}}{\mu}, \qquad \forall\, |x_1| < l, \tag{55}$$

has the following solution:

$$F_j''(z_j) = (-1)^k \frac{\dot{t}_{21}^{\infty}}{\mu} \frac{\beta_k \varepsilon_j}{\beta_2 \varepsilon_1^2 - \beta_1 \varepsilon_2^2} \left(1 - \frac{z_j}{\sqrt{z_j^2 - l^2}}\right), \quad j,k = 1,2, \quad j \neq k, \tag{56}$$

so that the perturbed stream function becomes

$$\psi^{\circ} = \frac{\dot{t}_{21}^{\infty}}{2\mu} \frac{\beta_2 \varepsilon_1}{\beta_2 \varepsilon_1^2 - \beta_1 \varepsilon_2^2} \sum_{j=1}^{2} \left(-\frac{\varepsilon_2 \beta_1}{\varepsilon_1 \beta_2}\right)^{j-1} \mathrm{Re}\left[z_j^2 - z_j\sqrt{z_j^2 - l^2} + l^2 \ln\left(z_j + \sqrt{z_j^2 - l^2}\right)\right], \tag{57}$$

and the incremental displacements take the form

$$\begin{aligned} v_1^{\circ} &= -\frac{\dot{t}_{21}^{\infty}}{\mu} \frac{\beta_1 \beta_2 \varepsilon_1}{\beta_2 \varepsilon_1^2 - \beta_1 \varepsilon_2^2} \mathrm{Im}\left[\left(z_1 - \sqrt{z_1^2 - l^2}\right) - \frac{\varepsilon_2}{\varepsilon_1}\left(z_2 - \sqrt{z_2^2 - l^2}\right)\right], \\ v_2^{\circ} &= -\frac{\dot{t}_{21}^{\infty}}{\mu} \frac{\beta_2 \varepsilon_1}{\beta_2 \varepsilon_1^2 - \beta_1 \varepsilon_2^2} \mathrm{Re}\left[\left(z_1 - \sqrt{z_1^2 - l^2}\right) - \frac{\beta_1 \varepsilon_2}{\beta_2 \varepsilon_1}\left(z_2 - \sqrt{z_2^2 - l^2}\right)\right]. \end{aligned} \tag{58}$$

Finally, for mode II in the EI regime, the incremental in-plane mean stress is given by

$$\dot{p}^{\circ} = -\dot{t}_{21}^{\infty} \frac{\beta_1 \beta_2 \varepsilon_1}{\beta_2 \varepsilon_1^2 - \beta_1 \varepsilon_2^2} \mathrm{Im}\left[\delta_1 \frac{z_1}{\sqrt{z_1^2 - l^2}} - \frac{\varepsilon_2 \delta_2}{\varepsilon_1} \frac{z_2}{\sqrt{z_2^2 - l^2}}\right], \tag{59}$$

while the incremental nominal stress components are

$$
\begin{aligned}
\dot{t}^{\circ}_{11} &= \dot{t}^{\infty}_{21}\frac{\beta_1\beta_2\varepsilon_1}{\beta_2\varepsilon_1^2-\beta_1\varepsilon_2^2}\mathrm{Im}\left[\varepsilon_1\frac{z_1}{\sqrt{z_1^2-l^2}}-\frac{\varepsilon_2^2}{\varepsilon_1}\frac{z_2}{\sqrt{z_2^2-l^2}}\right],\\
\dot{t}^{\circ}_{22} &= -\dot{t}^{\infty}_{21}\frac{\beta_1\beta_2\varepsilon_1\varepsilon_2}{\beta_2\varepsilon_1^2-\beta_1\varepsilon_2^2}\mathrm{Im}\left[\frac{z_1}{\sqrt{z_1^2-l^2}}-\frac{z_2}{\sqrt{z_2^2-l^2}}\right],\\
\dot{t}^{\circ}_{12} &= -\dot{t}^{\infty}_{21}\frac{\beta_1\beta_2\varepsilon_1\varepsilon_2}{\beta_2\varepsilon_1^2-\beta_1\varepsilon_2^2}\left\{\beta_1-\beta_2-\mathrm{Re}\left[\beta_1\frac{z_1}{\sqrt{z_1^2-l^2}}-\beta_2\frac{z_2}{\sqrt{z_2^2-l^2}}\right]\right\},\\
\dot{t}^{\circ}_{21} &= -\dot{t}^{\infty}_{21}\left\{1-\frac{\beta_2\varepsilon_1}{\beta_2\varepsilon_1^2-\beta_1\varepsilon_2^2}\mathrm{Re}\left[\varepsilon_1\frac{z_1}{\sqrt{z_1^2-l^2}}-\frac{\beta_1\varepsilon_2^2}{\beta_2\varepsilon_1}\frac{z_2}{\sqrt{z_2^2-l^2}}\right]\right\}.
\end{aligned}
\tag{60}
$$

Within the EC regime, eqns. (16), and for mode II, the Riemann-Hilbert problem:

$$
-2\left[\alpha(\delta^2-\chi^2)+2\beta\delta\chi\right]\mathrm{Re}\left[\frac{F_1''(x_1)}{(\alpha+i\beta)(\chi+i\delta)}\right]=\frac{\dot{t}^{\infty}_{21}}{\mu}, \qquad \forall\,|x_1|<l, \tag{61}
$$

has the following solution:

$$
F_j''(z_j)=-\frac{\dot{t}^{\infty}_{21}}{2\mu}\frac{[\alpha-(-1)^j i\beta][\chi-(-1)^j i\delta]}{\alpha(\delta^2-\chi^2)+2\beta\delta\chi}\left(1-\frac{z_j}{\sqrt{z_j^2-l^2}}\right), \quad j=1,2, \tag{62}
$$

so that the perturbed stream function becomes

$$
\begin{aligned}
\psi^{\circ}=-\frac{\dot{t}^{\infty}_{21}}{4\mu}\,\frac{1}{\alpha(\delta^2-\chi^2)+2\beta\delta\chi}\sum_{j=1}^{2}\mathrm{Re}\Big\{&[\alpha-(-1)^j i\beta][\chi-(-1)^j i\delta]\\
&\times\left[z_j^2-z_j\sqrt{z_j^2-l^2}+l^2\ln\left(z_j+\sqrt{z_j^2-l^2}\right)\right]\Big\},
\end{aligned}
\tag{63}
$$

and the incremental displacements take the form

$$
\begin{aligned}
v^{\circ}_1 &= \frac{\dot{t}^{\infty}_{21}}{2\mu}\frac{\alpha^2+\beta^2}{\alpha(\delta^2-\chi^2)+2\beta\delta\chi}\Big\{\chi\,\mathrm{Re}\left[\left(z_1-\sqrt{z_1^2-l^2}\right)-\left(z_2-\sqrt{z_2^2-l^2}\right)\right]\\
&\quad-\delta\,\mathrm{Im}\left[\left(z_1-\sqrt{z_1^2-l^2}\right)+\left(z_2-\sqrt{z_2^2-l^2}\right)\right]\Big\},\\
v^{\circ}_2 &= \frac{\dot{t}^{\infty}_{21}}{2\mu}\frac{1}{\alpha(\delta^2-\chi^2)+2\beta\delta\chi}\Big\{(\alpha\chi-\beta\delta)\,\mathrm{Re}\left[\left(z_1-\sqrt{z_1^2-l^2}\right)+\left(z_2-\sqrt{z_2^2-l^2}\right)\right]\\
&\quad-(\beta\chi+\alpha\delta)\,\mathrm{Im}\left[\left(z_1-\sqrt{z_1^2-l^2}\right)-\left(z_2-\sqrt{z_2^2-l^2}\right)\right]\Big\}.
\end{aligned}
\tag{64}
$$

Finally, for mode II in the EC regime, the incremental in-plane mean stress is given by

$$
\begin{aligned}
\dot{p}^{\circ} &= \frac{\dot{t}^{\infty}_{21}}{2}\frac{\alpha^2+\beta^2}{\alpha(\delta^2-\chi^2)+2\beta\delta\chi}\Big\{(\delta^2-k\chi)\,\mathrm{Re}\left[\frac{z_1}{\sqrt{z_1^2-l^2}}-\frac{z_2}{\sqrt{z_2^2-l^2}}\right]\\
&\quad+\delta(\chi+k)\,\mathrm{Im}\left[\frac{z_1}{\sqrt{z_1^2-l^2}}+\frac{z_2}{\sqrt{z_2^2-l^2}}\right]\Big\},
\end{aligned}
\tag{65}
$$

while the incremental nominal stress components are

$$
\begin{aligned}
\dot{t}^{\circ}_{11} &= \frac{\dot{t}^{\infty}_{21}}{2}\frac{\alpha^2+\beta^2}{\alpha(\delta^2-\chi^2)+2\beta\delta\chi}\left\{(\delta^2-\chi^2)\,\mathrm{Re}\left[\frac{z_1}{\sqrt{z_1^2-l^2}}-\frac{z_2}{\sqrt{z_2^2-l^2}}\right]\right. \\
&\quad \left. +\,2\delta\chi\,\mathrm{Im}\left[\frac{z_1}{\sqrt{z_1^2-l^2}}+\frac{z_2}{\sqrt{z_2^2-l^2}}\right]\right\}, \\
\dot{t}^{\circ}_{22} &= \frac{\dot{t}^{\infty}_{21}}{2}\frac{(\alpha^2+\beta^2)(\delta^2+\chi^2)}{\alpha(\delta^2-\chi^2)+2\beta\delta\chi}\,\mathrm{Re}\left[\frac{z_1}{\sqrt{z_1^2-l^2}}-\frac{z_2}{\sqrt{z_2^2-l^2}}\right], \\
\dot{t}^{\circ}_{12} &= -\frac{\dot{t}^{\infty}_{21}}{2}\frac{(\alpha^2+\beta^2)(\delta^2+\chi^2)}{\alpha(\delta^2-\chi^2)+2\beta\delta\chi}\left\{2\alpha-\alpha\,\mathrm{Re}\left[\frac{z_1}{\sqrt{z_1^2-l^2}}+\frac{z_2}{\sqrt{z_2^2-l^2}}\right]\right. \\
&\quad \left. -\,\beta\mathrm{Im}\left[\frac{z_1}{\sqrt{z_1^2-l^2}}-\frac{z_2}{\sqrt{z_2^2-l^2}}\right]\right\}, \\
\dot{t}^{\circ}_{21} &= \frac{\dot{t}^{\infty}_{21}}{2}\left\{-2+\mathrm{Re}\left[\frac{z_1}{\sqrt{z_1^2-l^2}}+\frac{z_2}{\sqrt{z_2^2-l^2}}\right]\right. \\
&\quad \left. -\,\frac{\beta(\delta^2-\chi^2)-2\alpha\delta\chi}{\alpha(\delta^2-\chi^2)+2\beta\delta\chi}\mathrm{Im}\left[\frac{z_1}{\sqrt{z_1^2-l^2}}-\frac{z_2}{\sqrt{z_2^2-l^2}}\right]\right\}.
\end{aligned}
\tag{66}
$$

Incremental stress intensity factors

We note that the incremental stress intensity factors, defined as

$$
\dot{K}_I = \lim_{x_1\to l^+}\frac{\dot{t}_{22}(x_1,x_2=0)}{\sqrt{2\pi\,(x_1-l)}},\quad \dot{K}_{II} = \lim_{x_1\to l^+}\frac{\dot{t}_{21}(x_1,x_2=0)}{\sqrt{2\pi\,(x_1-l)}}, \tag{67}
$$

follow immediately from the above calculations. These are

$$
\dot{K}_I = \dot{t}^{\infty}_{22}\sqrt{\pi l},\quad \dot{K}_{II} = \dot{t}^{\infty}_{21}\sqrt{\pi l}, \tag{68}
$$

for mode I and mode II loading, respectively. Note that, eqns. (68) coincide with their counterpart in elasticity without prestress, except that now the nominal stress replaces the Cauchy stress.

The crack solution and the surface bifurcation condition

The previously obtained crack solution remains valid except when the surface bifurcation condition, eqn. (22), is met. This condition corresponds to the two conditions

$$
\beta_2\varepsilon_1^2-\beta_1\varepsilon_2^2=0,\quad \alpha(\delta^2-\chi^2)+2\beta\delta\chi=0, \tag{69}
$$

valid in EI and EC, respectively. When the surface bifurcation condition is approached, the fields, solution of the crack problem, tend to blow up, a peculiarity first noted by Guz (1999, and references quoted therein).

For values of parameters ξ, k, and η beyond the surface instability threshold, the obtained solution still works, from a purely mathematical point of view. However, the crack faces cannot be maintained straight after a surface bifurcation point has been passed, so that the solution looses its physical meaning (the incremental energy release rate, obtained in Section 3.4, becomes negative in this situation).

3.2 Finite-length crack inclined with respect to the orthotropy axes

We consider now a crack inclined with respect to the x_1–x_2 axes defining the prestress directions and the orthotropy axes (see Fig. 3 of the paper, in which the shear band should be thought to represent a crack). Therefore, the x_1–x_2 reference system has to be distinguished from the system $\hat{x}_1$–$\hat{x}_2$, where the $\hat{x}_1$ axis is aligned parallel to the crack. The transformation between the two systems is expressed by eqn. (25), while the transformations between incremental displacement, its gradient, nominal stress and constitutive tensor are given by eqns. (26)–(28).

The trick to solve the inclined crack problem can be deduced from Savin (1961, see also Sih and Liebowitz, 1968) and consists in the introduction of a function analogous to (40) [see also eqns. (48), (57), and (63)], but now defined in the $\hat{x}_1$–$\hat{x}_2$ reference system, namely (which automatically satisfies the decaying conditions of fields at infinity)

$$\widehat{\psi}^{\circ}_M(\hat{x}_1, \hat{x}_2) = \frac{\hat{t}^{\infty}_{2n}}{2\mu} \sum_{j=1}^{2} \mathrm{Re}\left[A_j^M f(\hat{z}_j)\right], \tag{70}$$

where $n = 1$ and $M = II$ for mode II ($n = 2$ and $M = I$ for mode I), so that $\hat{t}^{\infty}_{21}$ ($\hat{t}^{\infty}_{22}$) is the traction component parallel (orthogonal) to the crack line. Moreover, $f(\hat{z}_j)$ is defined by

$$f(\hat{z}_j) = \hat{z}_j^{\,2} - \hat{z}_j \sqrt{\hat{z}_j^{\,2} - l^2} + l^2 \ln\left(\hat{z}_j + \sqrt{\hat{z}_j^{\,2} - l^2}\right), \tag{71}$$

where

$$\hat{z}_j = \hat{x}_1 + W_j\, \hat{x}_2, \qquad W_j = \frac{\sin\vartheta_0 + \Omega_j \cos\vartheta_0}{\cos\vartheta_0 - \Omega_j \sin\vartheta_0}. \tag{72}$$

Constants A_j^M in eqn. (70) can be obtained by imposing the boundary conditions on the crack faces, which are

$$\begin{aligned} &\bullet\quad \hat{t}^{\circ}_{21}(\hat{x}_1, 0^{\pm}) = 0, \qquad \hat{t}^{\circ}_{22}(\hat{x}_1, 0^{\pm}) = -\hat{t}^{\infty}_{22}, \quad \forall\, |\hat{x}_1| < l, \quad \text{for mode I;} \\ &\bullet\quad \hat{t}^{\circ}_{21}(\hat{x}_1, 0^{\pm}) = -\hat{t}^{\infty}_{21}, \quad \hat{t}^{\circ}_{22}(\hat{x}_1, 0^{\pm}) = 0, \qquad \forall\, |\hat{x}_1| < l, \quad \text{for mode II.} \end{aligned} \tag{73}$$

Imposing conditions (73) yields a linear algebraic system for the real and imaginary parts of constants A_j^M

$$\begin{bmatrix} c_{11} & c_{21} & c_{12} & c_{22} \\ -c_{21} & c_{11} & -c_{22} & c_{12} \\ c_{31} & c_{41} & c_{32} & c_{42} \\ -c_{41} & c_{31} & -c_{42} & c_{32} \end{bmatrix} \begin{bmatrix} \mathrm{Re}[A_1^M] \\ \mathrm{Im}[A_1^M] \\ \mathrm{Re}[A_2^M] \\ \mathrm{Im}[A_2^M] \end{bmatrix} = \underbrace{\begin{bmatrix} -1 \\ 0 \\ 0 \\ 0 \end{bmatrix}}_{\text{for mode I}} \text{ or } \underbrace{\begin{bmatrix} 0 \\ 0 \\ -1 \\ 0 \end{bmatrix}}_{\text{for mode II}}, \tag{74}$$

where $M = I$ for mode I ($M = II$ for mode II) and coefficients c_{ij} are

$$
\begin{aligned}
2\,\mu\, c_{1j} = \;& \widehat{\mathbb{K}}_{1112} - \widehat{\mathbb{K}}_{1222} - \mathrm{Re}[W_j]\left[\widehat{\mathbb{K}}_{1111} - 2\widehat{\mathbb{K}}_{1122} - \widehat{\mathbb{K}}_{1221} + \widehat{\mathbb{K}}_{2222}\right.\\
& \left. + \mathrm{Re}[W_j]\left(2\widehat{\mathbb{K}}_{1121} - 2\widehat{\mathbb{K}}_{2122} + \mathrm{Re}[W_j]\widehat{\mathbb{K}}_{2121}\right)\right]\\
& + \mathrm{Im}[W_j]^2\left(2\widehat{\mathbb{K}}_{1121} - 2\widehat{\mathbb{K}}_{2122} + 3\,\mathrm{Re}[W_j]\widehat{\mathbb{K}}_{2121}\right),\\
2\,\mu\, c_{2j} = \;& \mathrm{Im}[W_j]\left[\widehat{\mathbb{K}}_{1111} - 2\widehat{\mathbb{K}}_{1122} - \widehat{\mathbb{K}}_{1221} + \widehat{\mathbb{K}}_{2222}\right.\\
& \left. + \mathrm{Re}[W_j]\left(4\widehat{\mathbb{K}}_{1121} - 4\widehat{\mathbb{K}}_{2122} + 3\,\mathrm{Re}[W_j]\widehat{\mathbb{K}}_{2121}\right) - \mathrm{Im}[W_j]^2\widehat{\mathbb{K}}_{2121}\right],\\
2\,\mu\, c_{3j} = \;& -\widehat{\mathbb{K}}_{1221} + \mathrm{Re}[W_j]\left[\widehat{\mathbb{K}}_{1121} - \widehat{\mathbb{K}}_{2122} + \mathrm{Re}[W_j]\widehat{\mathbb{K}}_{2121}\right) - \mathrm{Im}[W_j]^2\widehat{\mathbb{K}}_{2121},\\
2\,\mu\, c_{4j} = \;& \mathrm{Im}[W_j]\left(-\widehat{\mathbb{K}}_{1121} + \widehat{\mathbb{K}}_{2122} - 2\,\mathrm{Re}[W_j]\widehat{\mathbb{K}}_{2121}\right), \quad j = 1, 2,
\end{aligned}
\tag{75}
$$

and depend on the crack inclination ϑ_0 and on the prestress and orthotropy parameters ξ, k and η.

The determinant of the coefficient matrix in eqn. (74) is null only when the surface instability condition, eqn. (22), is met, so that in all other cases, system (74) can be solved and the solution of the inclined crack follows.

The perturbed incremental displacement along the crack faces can be obtained in the form

$$
\begin{aligned}
\hat{v}_1^{\circ M}(\hat{x}_1, \hat{x}_2 = 0^{\pm}) &= \frac{\hat{t}_{2n}^{\infty}}{2\mu}\mathrm{Re}\left[(W_1 A_1^M + W_2 A_2^M)\left(\hat{x}_1 \mp i\sqrt{l^2 - \hat{x}_1^2}\right)\right],\\
\hat{v}_2^{\circ M}(\hat{x}_1, \hat{x}_2 = 0^{\pm}) &= -\frac{\hat{t}_{2n}^{\infty}}{2\mu}\mathrm{Re}\left[(A_1^M + A_2^M)\left(\hat{x}_1 \mp i\sqrt{l^2 - \hat{x}_1^2}\right)\right],
\end{aligned}
\tag{76}
$$

so that the jump in incremental displacements across the crack surfaces ($\hat{x}_2 = 0$, $|\hat{x}_1| < l$) takes the form

$$
\begin{aligned}
[[\hat{v}_1^M]] &= \frac{\hat{t}_{2n}^{\infty}}{\mu}\mathrm{Im}[W_1 A_1^M + W_2 A_2^M]\sqrt{l^2 - \hat{x}_1^2},\\
[[\hat{v}_2^M]] &= -\frac{\hat{t}_{2n}^{\infty}}{\mu}\mathrm{Im}[A_1^M + A_2^M]\sqrt{l^2 - \hat{x}_1^2},
\end{aligned}
\tag{77}
$$

where $n = 1$ and $M = II$ ($n = 2$ and $M = I$) for mode II (mode I).

It is worth noting that the following conditions, proven in the particular cases of null prestress or crack parallel to the orthotropy axes, have been in general verified numerically to hold

$$
\mathrm{Re}[A_1^I + A_2^I] = 0, \qquad \mathrm{Re}[W_1 A_1^{II} + W_2 A_2^{II}] = 0,
\tag{78}
$$

showing that the incremental perturbed displacement along the x_1-axis outside the crack is only longitudinal, i.e. $\hat{v}_2^{\circ} = 0$, (transversal, i.e. $\hat{v}_1^{\circ} = 0$,) for mode I (for mode II), a circumstance noted also by Broberg (1999, his section 4.14) for infinitesimal anisotropic elasticity.

In addition to eqns. (78), the following conditions are obtained in the particular case of a crack parallel to the orthotropy x_1-axis, $\vartheta_0 = 0$,

$$\mathrm{Im}[W_1 A_1^I + W_2 A_2^I] = 0, \quad \mathrm{Im}[A_1^{II} + A_2^{II}] = 0, \tag{79}$$

from which the solution obtained in Section 3.1 can be easily recovered.

Finally, *the incremental stress intensity factors for an inclined crack can be calculated and again result in the form* (68), *found for a crack parallel to the orthotropy axes.*

The inclined crack solution becomes particularly simple in the case when the prestress is null, $k = \eta = 0$. In particular, for mode I we have:

$$A_j^I = -(-1)^j \frac{\cos 2\vartheta_0}{2\sqrt{1-\xi}} - i\,\frac{1-\xi-(-1)^j\sqrt{1-\xi}\sin 2\vartheta_0}{2(1-\xi)\sqrt{\xi}}, \quad j = 1, 2, \tag{80}$$

while for mode II:

$$A_j^{II} = (-1)^j \left[\frac{\sin 2\vartheta_0}{2\sqrt{1-\xi}} + i\,\frac{\cos 2\vartheta_0}{2\sqrt{(1-\xi)\xi}}\right], \quad j = 1, 2, \tag{81}$$

The following properties can also be proven

$$W_1 A_1^I + W_2 A_2^I = 0, \quad A_1^{II} + A_2^{II} = 0. \tag{82}$$

An interesting feature that does not hold when the prestress is present and the crack is inclined can be deduced from eqns. (77), $(82)_1$ and (81), namely, that a mode I (mode II) loading does not produce longitudinal, v_1, (transversal, v_2,) incremental displacements along the crack line, so that for $\hat{x}_2 = 0$ and $|\hat{x}_1| < l$, we have

$$[[\hat{\mathbf{v}}]] = \left\{ \frac{\hat{t}_{21}^\infty}{\mu\sqrt{\xi}}\sqrt{l^2 - \hat{x}_1^2}, \; \frac{\hat{t}_{22}^\infty}{\mu\sqrt{\xi}}\sqrt{l^2 - \hat{x}_1^2} \right\}, \tag{83}$$

which is independent of the crack inclination ϑ_0.

As an example of the previous calculations, the deformed crack line and surfaces (incremental displacement components, reported on the vertical axis for $\hat{v}_2$ and on the horizontal axis for $\hat{x}_1 + \hat{v}_1$, are normalized through division by l) for mode I (left) and mode II (right) loading at infinity are illustrated in Fig. 3 for a Mooney-Rivlin material ($\xi = 1$) at null prestress $k = 0$ and at $k = 0.8$ for a crack parallel to the orthotropy x_1-axis, i.e. $\vartheta_0 = 0$, and inclined at $\vartheta_0 = \pi/6$. Note that the mode II deformation at null prestress, $k = 0$ coincides with the horizontal axis and is therefore not visible.

Interesting features emerging from Fig. 3 are: i.) the crack faces result displaced to the shape of an ellipse; ii.) this ellipse degenerates into a segment for mode II and null prestress; iii.) the prestress introduces an incremental rigid-body rotation in the mode I and mode II solutions.

3.3 Shear bands interacting with a finite-length crack

In the spirit of the perturbative approach proposed by Bigoni and Capuani (2002; 2005), the role of shear banding in the incremental deformation fields

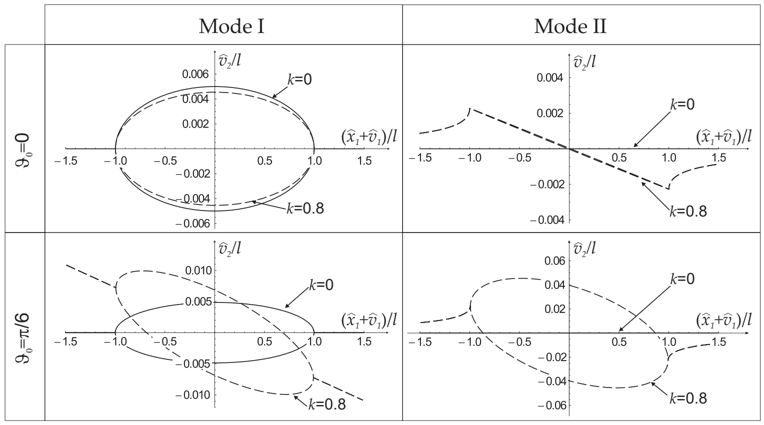

Figure 3: Deformed shape of a crack of length $2l$, subject to mode I (left) and mode II (right) incremental loading ($\hat{t}_{22}^{\infty}/\mu = 0.01$ and $\hat{t}_{21}^{\infty}/\mu = 0.01$). A Mooney-Rivlin material is considered with null prestress $k = 0$ (solid curve) and a prestress defined by $k = 0.8$ (dashed curve). A crack is parallel to the x_1-orthotropy axis, $\vartheta_0 = 0$ (upper part), while a second crack is inclined at an angle $\vartheta_0 = \pi/6$ (lower part).

around a crack of length $2l$ is investigated. This crack is assumed to be present in the material with a dead loading on its surfaces to maintain the state of prestress, before the incremental mode I and II loadings are assigned.

The crack is considered in a J_2-deformation theory material, inclined at an angle corresponding to the shear band inclination at the EC/H boundary. In particular, for the two values of hardening exponent $N = 0.1$ and $N = 0.8$, the critical logarithmic strain for localization (and the shear band inclination with respect to x_1-axis) are $\varepsilon \approx 0.322$ ($\vartheta_0 \approx 35.95°$) and $\varepsilon \approx 1.032$ ($\vartheta_0 \approx 19.60°$), respectively. (Note that for a J_2–deformation theory material the prestrain, instead than the prestress, is used as the parameter controlling the current state).

The level sets of the modulus of incremental deviatoric strain have been mapped in Figs. 4 and 5, for low strain hardening $N = 0.1$ and high strain hardening $N = 0.8$, respectively.

The investigation has been carried out with a choice of η, namely, $\eta/k = 0.311$ for $N = 0.1$ and $\eta/k = 0.775$ for $N = 0.8$, such that the Hill exclusion condition (4) is satisfied.

It can be easily concluded from Figs. 4 and 5 that:

> *near the elliptic border the deformation fields become highly focused and aligned parallel to the shear band conjugate directions.*

An analysis of the figures reveals that it becomes difficult to predict how the fracture will grow when loaded near the elliptic border. However, we have to keep in mind that the analysed crack has been taken aligned parallel to one shear band direction. It becomes instructive now to analyse the case of a horizontal crack (lying therefore in a symmetry axis with respect to the conjugate band directions), reported in Fig. 6, for a J_2–deformation theory material at high strain hardening $N = 0.8$, near the EC/H boundary, and loaded under

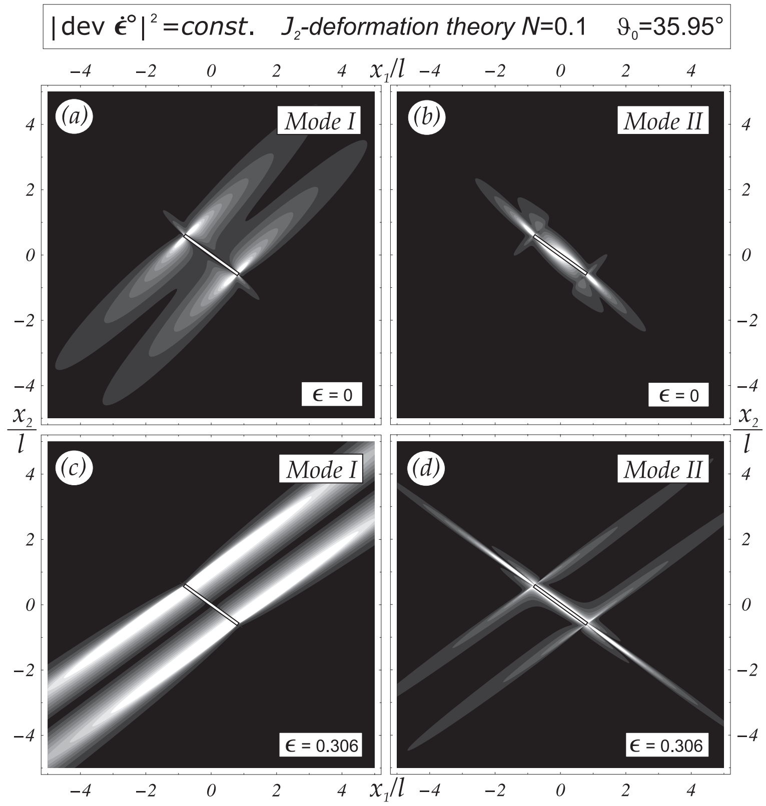

Figure 4: Interaction of shear bands and mechanical fields near a crack of length $2l$. A J_2–deformation theory material has been considered at low strain hardening $N = 0.1$, at null prestrain $\varepsilon = 0$ (upper part) and prestrained near the elliptic border $\varepsilon = 0.306$ (lower part). The crack is aligned parallel to a shear band direction, $\vartheta_0 = 35.95°$. Two parallel bands emerge for mode I incremental loading, while for mode II two conjugate band directions are visible.

incremental mode I. Results are qualitatively analogous for different values of strain hardening and for mode II loading, in particular, the mode II incremental deformation fields are dominated near the elliptic border by localized deformations aligned parallel to the two shear bands conjugate directions, in a way quite similar to Fig. 6.

We can observe that:

two symmetric shear bands emerge near the crack tip,

and their interaction may lead to failure of the material under shear in front of the crack, a situation compatible with mode I growth, to be interpreted as a sort of 'alternating sliding off and cracking', as suggested by McClintock (1971) and Kardomateas and McClintock (1989). The situation is more complicated for mode II loading, but our results agree with the consideration made by Hallbäck and Nilsson (1994), that 'mode II failure results when the direction of the prospective shear band coincides with the crack surface direction, while mode I type failure occurs when the shear bands are inclined to the direction of crack surfaces.'

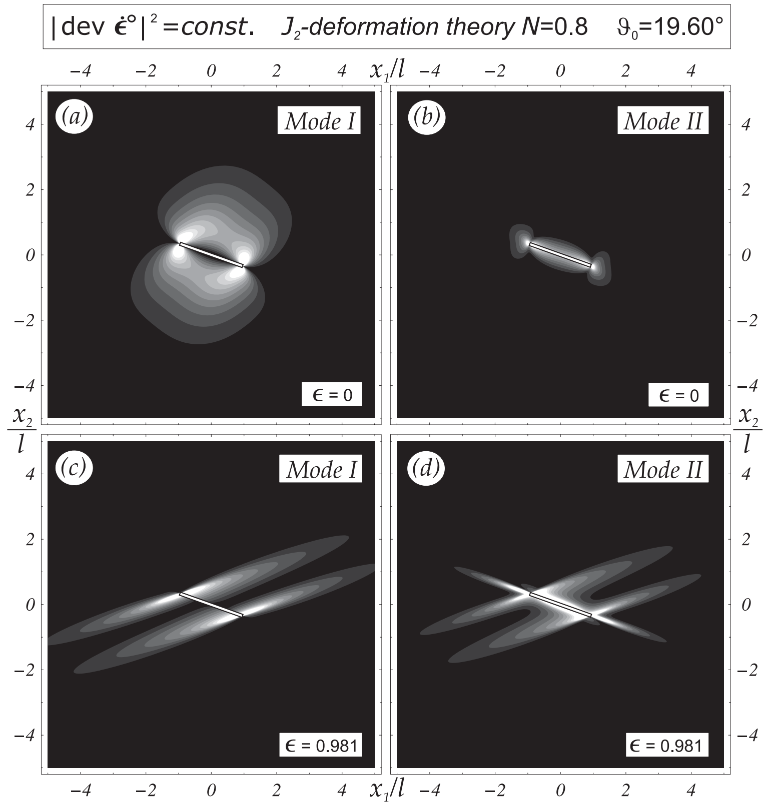

Figure 5: Interaction of shear bands and mechanical fields near a crack of length $2l$. A J_2–deformation theory material has been considered at high strain hardening $N = 0.8$, at null prestrain $\varepsilon = 0$ (upper part) and prestrained near the elliptic border $\varepsilon = 0.981$ (lower part). The crack is aligned parallel to a shear band direction, $\vartheta_0 = 19.60°$. Two parallel bands emerge for mode I incremental loading, while for mode II two conjugate band directions are visible.

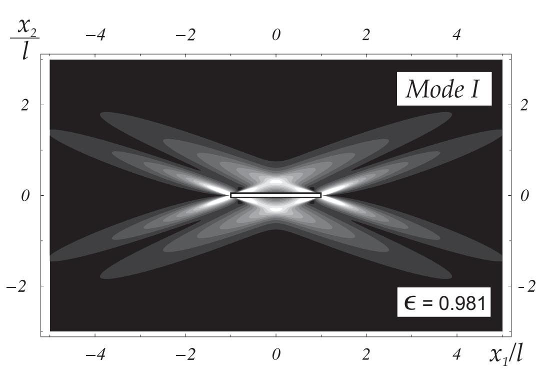

Figure 6: Interaction of shear bands and mechanical fields near a crack of length $2l$ under mode I incremental loading. A J_2–deformation theory material has been considered at high strain hardening $N = 0.8$, prestrained near the elliptic border $\varepsilon = 0.981$. The crack is horizontal, while the shear bands are inclined at $\pm 19.60°$. Note that four shear bands emerge.

3.4 Incremental energy release rate for crack growth

We slightly generalize Rice (1968) and start referring to Fig. 7 and comparing two incremental boundary value problems (for finite bodies subject to identical conditions on the external boundaries $S_\sigma \cup S_v$, namely, prescribed incremental nominal tractions $\dot{\boldsymbol{\sigma}}^0$ on S_σ and incremental displacements $\mathbf{v} = \bar{\mathbf{v}}$ on S_v) differing only in the sizes of the void that they contain. Note that we are addressing an incremental problem, so that the surface of the void can be loaded by dead loading.

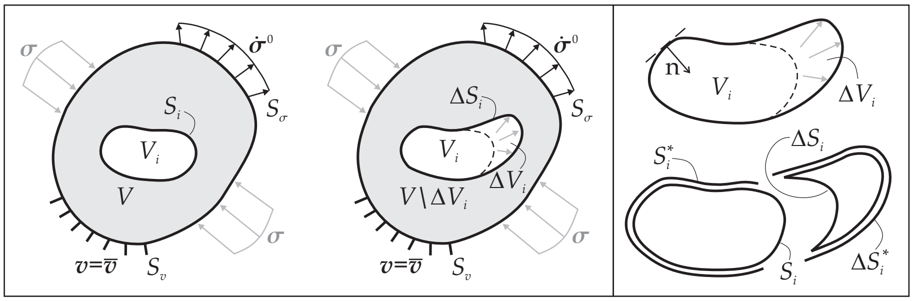

Figure 7: Two elastic, prestressed bodies are compared (left), having identical shape, boundary conditions, elastic properties, prestress, and prestrain, but voids of different size. The detail of the void and its surface is reported on the right; note the unit normal vector, defined to point outward the elastic body and toward the void. Incremental deformation of prestressed solids are considered, so that the surface of the void can be subject to finite dead loading and surface ΔS_i^* must be subject to the nominal tractions present on the same surface embedded in the material in the configuration on the left.

In particular, the void in the body on the right (of volume $V_i \cup \Delta V_i$, enclosed by surface $S_i^* \cup \Delta S_i^*$) has been obtained by increasing the size of the void in the body on the left (of volume V_i, enclosed by surface S_i).

Since we want to include prestress in an incremental formulation, nominal (finite) dead tractions identical to those existing within the material containing the void V_i must be applied on the surface ΔS_i^* of the material containing the void $V_i \cup \Delta V_i$.

We define the incremental displacement and nominal traction fields, solutions to the two problems, as $\mathbf{v}^0$ and $\dot{\mathbf{t}}^0$ for the problem on the left and $\mathbf{v} = \mathbf{v}^0 + \tilde{\mathbf{v}}$ and $\dot{\mathbf{t}} = \dot{\mathbf{t}}^0 + \tilde{\mathbf{t}}$ for the problem on the right. Since the void surfaces are subject to dead loading, $\dot{\mathbf{t}}^{0T}\mathbf{n} = \mathbf{0}$ and $\dot{\mathbf{t}}^T\mathbf{n} = \mathbf{0}$, within V_i and $V_i \cup \Delta V_i$, respectively.

The two bodies are assumed to be identically prestressed and prestrained, although not necessarily in a homogeneous way. If the expedient of prescribing 'ad hoc' dead tractions on ΔS_i^* is not considered and the void surface is free of tractions, in order to have identical prestress and prestrain, the two current configurations shown in Fig. 7 must have special geometries and loadings, as will be the case of a crack aligned parallel to a principal stress direction with the other principal stress to be null and, more important, of our shear band model (Section 3 of the paper).

The incremental potential energy decrease for a void growth in an elastic (incompressible or compressible, generically anisotropic and prestressed) body, takes an expression analogous to that reported by Rice [1968, his eqn. (55), pp. 207], namely,

$$-\Delta \dot{P} = \int_{\Delta V_i} \phi(\nabla \mathbf{v}^0) dV - \frac{1}{2}\int_{\Delta S_i^*} \mathbf{n} \cdot \mathbf{t}^0 \tilde{\mathbf{v}} dS, \tag{84}$$

a quantity which when positive, implies void *growth.* Note that the scalar function ϕ is the incremental gradient potential defined as

$$\dot{t}_{ij} = \frac{\partial \phi(\nabla \mathbf{v})}{\partial v_{j,i}} + \dot{p}\,\delta_{ij}, \quad \phi(\nabla \mathbf{v}) = \frac{1}{2} v_{j,i} \mathbb{K}_{ijhk} v_{k,h}. \tag{85}$$

Turning now the attention to a thin void inclusion, namely, a crack aligned parallel to the $\hat{x}_1$–axis (Fig. 2), the volume integral in eqn. (84) vanishes, so that taking the limit of the length increase $\Delta l \to 0$ at fixed incremental stress intensity factor $\dot{K}$, eqn. (84) becomes

$$\dot{G} = -\frac{d\dot{P}}{dl} = \lim_{\Delta l \to 0} \frac{1}{2\Delta l} \int_0^{\Delta l} \hat{t}_{2i}(r,0)[[\hat{v}_i(\Delta l - r, \pi)]]\, dr, \tag{86}$$

where the symbol $\hat{\cdot}$ denotes that we are using the inclined crack solution, the repeated index is summed, r denotes the radial distance from the crack tip and 0 and π indicate values of the polar coordinate (anticlockwise) angle singling out r from the $\hat{x}_1$ axis (so that $\theta = 0$ corresponds to points ahead of the crack tip). Eqn. (86) defines

> *the incremental energy release rate for a mixed mode growth of a crack in an elastic, incompressible or compressible body, generically anisotropic and prestressed.*

The proof that the incremental energy release rate coincides with the path–independent incremental $\dot{J}$–integral

$$\dot{J} = \int_\Gamma \left(\hat{\phi}\, \hat{n}_1 - \hat{n}_j \hat{t}_{ji} \frac{\partial\, \hat{v}_i}{\partial\, \hat{x}_1} \right) d\Gamma, \tag{87}$$

has not yet been explicitly obtained, but the validity of $\dot{G} = \dot{J}$ has been verified numerically.

The incremental energy release rate (86) can be developed making use of the asymptotic near-tip incremental nominal stress ahead of the crack

$$\hat{t}_{22}(r,0) = \frac{\dot{K}_I}{\sqrt{2\pi r}}, \qquad \hat{t}_{21}(r,0) = \frac{\dot{K}_{II}}{\sqrt{2\pi r}}, \tag{88}$$

and incremental displacement on the crack faces (where constants have been neglected)

$$\begin{aligned} \hat{v}_1(\Delta l - r, \pm\pi) &= \pm \frac{\sqrt{2l}\sqrt{\Delta l - r}}{2\mu} \mathrm{Im}\left[\hat{t}_{22}^{\infty}(W_1 A_1^I + W_2 A_2^I) + \hat{t}_{21}^{\infty}(W_1 A_1^{II} + W_2 A_2^{II}) \right], \\ \hat{v}_2(\Delta l - r, \pm\pi) &= \mp \frac{\sqrt{2l}\sqrt{\Delta l - r}}{2\mu} \mathrm{Im}\left[\hat{t}_{22}^{\infty}(A_1^I + A_2^I) + \hat{t}_{21}^{\infty}(A_1^{II} + A_2^{II}) \right], \end{aligned} \tag{89}$$

holding for 'small' Δl.

Employing the asymptotic near-tip representations (88) and (89) in eqn. (86) we obtain

$$
\begin{aligned}
\dot{G} = \; & -\dot{K}_I^2 \frac{\operatorname{Im}\left[A_1^I + A_2^I\right]}{4\mu} + \dot{K}_{II}^2 \frac{\operatorname{Im}\left[W_1 A_1^{II} + W_2 A_2^{II}\right]}{4\mu} \\
& + \dot{K}_I \dot{K}_{II} \frac{\operatorname{Im}\left[W_1 A_1^I + W_2 A_2^I - A_1^{II} - A_2^{II}\right]}{4\mu},
\end{aligned}
\tag{90}
$$

representing the incremental energy release rate for an inclined crack loaded in mixed mode in a prestressed, orthotropic and incompressible material.

From eqn. (90) *the incremental energy release rate for a mixed mode loading of a crack parallel to the orthotropy axes* (i.e. $\vartheta_0 = 0$) can be made explicit

$$
\dot{G} = \frac{\Lambda}{\mu} \frac{\dot{K}_I^2 \sqrt{1-k} + \dot{K}_{II}^2 \sqrt{1+k}}{(2\xi - \eta + \Lambda)^2 \sqrt{2\xi - 1 - \Lambda} - (2\xi - \eta - \Lambda)^2 \sqrt{2\xi - 1 + \Lambda}},
\tag{91}
$$

where there is no coupling between the two modes I and II.

Another interesting special case is that of null prestress, in which for an inclined crack the following expression of the incremental energy release rate can be obtained

$$
\dot{G} = \frac{\dot{K}_I^2 + \dot{K}_{II}^2}{4\mu\sqrt{\xi}},
\tag{92}
$$

which agrees with the known isotropic elasticity solution in the incompressible limit, recovered for $\xi = 1$.

Note that both incremental energy release rates (90) and (91) generally (an exception to this rule will be shown in Fig. 8) blow up to infinity when the surface bifurcation, eqn. (22) or (69), is approached, as in the case of the crack aligned parallel to one of the orthotropy axes. This feature is evident in the example reported below.

An example of calculation of incremental energy release rate for inclined (at $\vartheta_0 = \{0, \pi/4, \pi/2\}$) mode I and a mode II cracks in an incrementally isotropic material ($\xi = 1$) as a function of the prestress parameter k is reported in Fig. 8, where $\dot{G}$ has been normalized through division by $\dot{K}_M^2$ and multiplication by 4μ. In order to explore the incremental energy release rate until close to the elliptic boundary (more precisely, to the EI/P boundary), we have taken $\eta = k > 0$, so that the Hill condition (4) excludes all possible bifurcations within EI. It may be interesting to observe from Fig. 8 that, with the exceptions of $\vartheta_0 = 0$ for mode I and $\vartheta_0 = \pi/2$ for mode II, the incremental energy release rate blows up to infinity when k approaches 1. These exceptions can be motivated by the circumstance that at the EI/P boundary only one shear band forms aligned parallel to the major principal (tensile in this case) stress component, σ_1. Therefore, for mode I (mode II) a crack parallel (orthogonal) to the shear

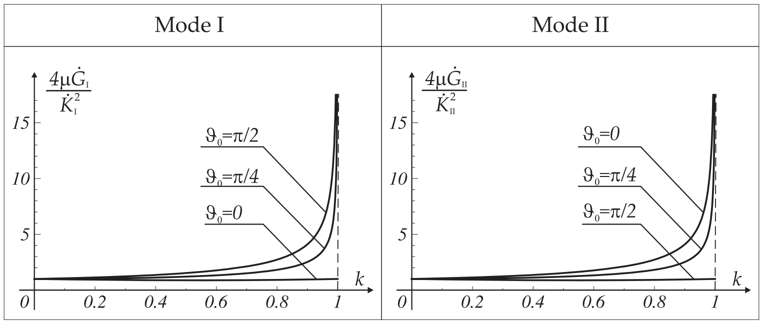

Figure 8: Incremental stress release rate for a mode I and mode II cracks of length $2l$ inclined at $\vartheta_0 = \{0, \pi/4, \pi/2\}$ with respect to the principal stress axis $\hat{x}_1$ in an incrementally isotropic material ($\xi = 1$) as a function of the prestress parameter k, taken positive and equal to η, so that the Hill exclusion criterion (4) is satisfied.

band is not influenced by the progressive weakening in the shear band direction occurring when the elliptic boundary is approached.

Note that for a Mooney-Rivlin material μ is a function of k, blowing up to infinity, when the EI/P boundary ($k = 1$) is approached. As a consequence, for a Mooney-Rivlin material the energy release rate remains finite when k tends to 1.

Note that for null prestress, $\eta = k = 0$, eqn. (92) shows that the incremental energy release rate blows up to infinity when ξ tends to zero, which corresponds to the EC/H boundary and to the appearance of the two shear bands inclined at $\pi/4$ with respect to the principal stress direction, typical of Mises plasticity.

Fig. 8 reveals another interesting feature, namely, that the curves corresponding to $\vartheta_0 = \{0, \pi/4, \pi/2\}$ in mode I are identical to the curves corresponding, respectively, to $\vartheta_0 = \{\pi/2, \pi/4, 0\}$ in mode II. More in general, the following relation can be proven in the absence of prestress using eqns. (80) and (81)

$$\frac{\dot{G}_I(\vartheta_0)}{\dot{K}_I^2} = \frac{\dot{G}_{II}(\pi/2 - \vartheta_0)}{\dot{K}_{II}^2}, \tag{93}$$

and has been numerically found to hold also when the prestress is different from zero.

References

[1] Bigoni, D. and Capuani, D. 2002 Green's function for incremental nonlinear elasticity: shear bands and boundary integral formulation. *J. Mech. Phys. Solids* **50**, 471-500.

[2] Bigoni, D. and Capuani, D. 2005 Time-harmonic Green's function and boundary integral formulation for incremental nonlinear elasticity: dynamics of wave patterns and shear bands. *J. Mech. Phys. Solids* **53**, 1163-1187.

[3] Biot, M.A. 1965 *Mechanics of incremental deformations.* J. Wiley and Sons, New York.

[4] Broberg, K.B. 1999 *Cracks and fracture.* Academic Press, San Diego, CA, USA.

[5] Cristescu, N.D., Craciun, E.M. and Soós, E. 2004 *Mechanics of elastic composites.* Chapman & Hall/CRC, Boca Raton.

[6] Dal Corso, F., Bigoni, D. and Gei, M. 2008 The stress concentration near a rigid line inclusion in a prestressed, elastic material. Part I. Full-field solution and asymptotics. *J. Mech. Phys. Solids* **56**, 815-838.

[7] Guz, A. N. 1999 *Fundamentals of the three-dimensional theory of stability of deformable bodies*, Springer-Verlag, Berlin.

[8] Hallbäck, N. and Nilsson, F. 1994 Mixed-mode I/II fracture behaviour of an Aluminium alloy. *J. Mech. Phys. Solids* **42**, 1345-1374.

[9] Hill, R. 1958 A general theory of uniqueness and stability in elastic-plastic solids. *J. Mech. Phys. Solids* **6**, 236-249.

[10] Hill, R. and Hutchinson, J.W. 1975 Bifurcation phenomena in the plane tension test. *J. Mech. Phys. Solids* **23**, 239-264.

[11] Hutchinson, J.W. and Neale, K.W., 1979 Finite strain J2-deformation theory. In *Proc. IUTAM Symp. on Finite Elasticity*, D.E. Carlson and R.T. Shield Eds., Martinus Nijhoff, The Hague-Boston-London, pp. 237-247.

[12] Kardomateas, G.A. and McClintock, F.A. 1989 Shear band characterization of mixed mode I and II fully plastic crack growth. *Int. J. Fracture* **40**, 1-12.

[13] Lekhnitskii, S.G. 1981 *Theory of Elasticity of an Anisotropic Body.* Mir Publisher, Moscow.

[14] McClintock, F.A. 1971 Plasticity aspects of fracture. In: '*Fracture. An Andvanced Treatise*', H. Liebowitz Editor, Vol. **III**, Academic press Inc., New York, 47-225.

[15] Needleman, A. and Ortiz, M. 1991 Effects of boundaries and interfaces on shear-band localization. *Int. J. Solids Structures* **28**, 859-877.

[16] Radi, E., Bigoni, D. and Capuani, D. 2002 Effects of prestress on crack-tip fields in elastic, incompressible solids. *Int. J. Solids Structures* **39**, 3971-3996.

[17] Rice, J.R. 1968 Mathematical analysis in the mechanics of fracture. In: '*Fracture. An Andvanced Treatise*', H. Liebowitz Editor, Vol. **II**, Academic press Inc., New York, pp. 191-311.

[18] Savin, G.N. 1961 *Stress Concentration around Holes.* Pergamon Press, Oxford, London.

[19] Sih, G.C. and Liebowitz, H. 1968 In: 'Fracture. An Andvanced Treatise', H. Liebowitz Editor **II**, 67.